

MODELING OF THE THREE-BODY EFFECTS IN THE NEUTRAL TRIMERS IN THE QUARTET STATE BY *ab initio* CALCULATIONS. H₃, Na₃, AND Na₂B

Jacek JAKOWSKI^{a1,+}, Grzegorz CHAŁASIŃSKI^{a2,*,+}, Małgorzata M. SZCZEŚNIAK^b
and Sławomir M. CYBULSKI^c

^a Faculty of Chemistry, University of Warsaw, Pasteura 1, 02-093 Warsaw, Poland;
e-mail: ¹ jakow@chem.uw.edu.pl, ² chalbie@chem.uw.edu.pl

^b Department of Chemistry, Oakland University, Rochester, MI 48309, U.S.A.;
e-mail: maria@ouchem.chem.oakland.edu

^c Department of Chemistry, Miami University, Oxford, OH 45056, U.S.A.;
e-mail: cybulssm@muohio.edu

Received August 12, 2002
Accepted November 11, 2002

Dedicated to Professors Petr Čársky, Ivan Hubač and Miroslav Urban:

*"In the mustardseed sun,
By full tilt river and switchback sea
Where the cormorants scud,
In their house on stilts high among beaks
And palavers of birds
This sandgrain day in the bent bay's grave
They celebrate and spurn
their driftwood sixtieth wind turned age;
herons spire and spear."*

(Dylan Thomas)

The Na₂B, Na₃, and H₃ trimers in the lowest quartet states were studied by *ab initio* methods, using both the supermolecular approach and the intermolecular Møller-Plesset perturbation theory. Partitioning of the nonadditive contribution into the orientational two-body part and the genuine three-body part was proposed. The lowest quartet state of the Na₃ trimer and all the three lowest quartet states of the Na₂B trimer are bound, and the forms of these clusters are essentially determined by two-body forces. In the case of the Na₂B trimer the orientational two-body nonadditivity proved to be crucial. In addition, in the title metal trimers, in the region of the van der Waals minima, the genuine nonadditivity is very important, and amounts to 30% in Na₂B and up to 70% in Na₃. The leading nonadditive term

+ Presently at Chemistry Department, University of Utah, Salt Lake City, UT 84112, U.S.A.
++Also at Department of Chemistry, Oakland University, Rochester, MI 48309, U.S.A.

is the triple-exchange Heitler–London exchange term. For triangular arrangements it considerably enhances the total stabilization. The single-exchange term and the SCF deformation play only a secondary role. The dispersion nonadditivity is negligible. The isotropic part of the basis set superposition error (BSSE) is large and must be corrected by the counterpoise method. The anisotropic contribution to BSSE is practically negligible.

Keywords: Perturbation theory, Counterpoise method; Sodium; Hydrogen; Trimers; *Ab initio* calculations; Clusters.

Recently, increasing experimental and theoretical efforts have been devoted to study the interaction of metal atoms^{1–9}. The alkali metal complexes have been extensively studied by Gutowski and co-workers^{6,8,10,11}. Boron, which is a prototype of the IIIA group, has been studied by Alexander, Dagdigian and their collaborators^{12–17}.

Our interest in the three-body forces in the quartet state neutral trimers stems from the fact that recent theoretical and experimental results for Na₃^{10,11} suggested a critical role for the nonadditive forces in stabilizing the trimer. According to Higgins *et al.*¹¹, the A₂' Na₃ potential energy surface is characterized by a D_{3h} symmetry minimum of –850 cm^{–1} (relative to the three ground state ²S Na atom dissociation limit) with the bond distance of 4.406 Å. This bond distance differs by about 0.8 Å from the value of 5.2 Å found for the sodium triplet dimer. The three-body effect thus amounts to –694 cm^{–1}, and accounts for almost 80% of the well depth of the trimer! The authors stipulated that “this large three-body contribution is caused by the decreased overlap repulsion of the electrons in the trimer which is due to the highly deformable valence electron shells of the interacting sodium atoms”. In the language of the symmetry adapted perturbation theory (SAPT) of intermolecular interactions^{18–20}, this is the exchange nonadditivity which is responsible for the huge extra stabilization and sizeable shrinking of the trimer. There are several exchange nonadditive mechanisms which can produce three-body contributions of a different character. It is of great interest to find out what mechanism dominates the total exchange nonadditive effect.

The striking behavior of the quartet state of Na₃ motivated us to study another candidate likely to reveal an important three-body effect, the yet undiscovered Na₂B trimer. The quartet state Na₂B trimer with the valence 2s_B² 2p_B¹ 3s_{Na1}¹ 3s_{Na2}¹ electron configuration represents a simple model to study the anisotropy of the three-body exchange terms and other nonadditive contributions originating from a singly occupied p-symmetry orbital of boron. It is also the simplest model of a metallic cluster with an impurity.

Such clusters have recently been studied by several groups, as amply documented by Alonso and Lopez²¹.

The interaction of two (²S) Na and (²P) B in the isosceles triangle form leads to three different orientations of the singly occupied p orbital in the Na₂B trimer: a₁, b₁, and b₂ of the C_{2v} point group symmetry (Fig. 1). The 3s orbitals of the two Na atoms generate two singly occupied molecular orbitals, a₁ and b₂. As a consequence of three possible orientations of the p orbital, three different states of the Na₂B arise: B₂, A₂, and A₁, which relate respectively to a₁, b₁, and b₂ orientations of p orbital.

In the supermolecular approach, the interaction energy of the trimer is calculated as the difference between the energy of the complex and the monomer energies

$$E_{\text{int}}(\text{ABC}) = E(\text{ABC}) - E(\text{A}) - E(\text{B}) - E(\text{C}) , \quad (1)$$

where $E(\text{ABC})$ is the trimer energy, and $E(\text{A})$, $E(\text{B})$, and $E(\text{C})$ are monomer energies. $E_{\text{int}}(\text{ABC})$ may be expressed as the sum of two-body (pair) interactions and a three-body nonadditive effect:

$$E_{\text{int}}(\text{ABC}) = E[2,3] + E[3,3] , \quad (2)$$

where

$$E[2,3] = E_{\text{int}}(\text{AB}) + E_{\text{int}}(\text{BC}) + E_{\text{int}}(\text{AC}) \quad (3)$$

$$E_{\text{int}}(\text{XY}) = E(\text{XY}) - E(\text{X}) - E(\text{Y}) \quad (4)$$

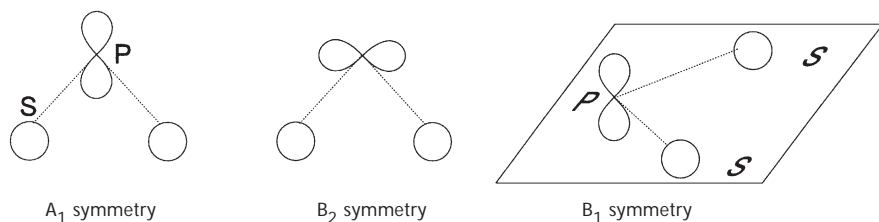


FIG. 1

Orientation of the p singly occupied orbital of the B atom in the Na₂B-like trimers for isosceles geometries (the C_{2v} point group). In the B₁ symmetry the p orbital is perpendicular to the Na₂B plane

and the three-body part is defined recursively

$$E[3,3] = E_{\text{int}}(\text{ABC}) - E[2,3] . \quad (5)$$

Equations which include subtractions of the energies of monomers, dimers, and the trimer require consistent evaluation:

1. The energies of monomers, dimers, and the trimer should be calculated at the same level of theory. In particular, the method must be size consistent. This condition is fulfilled if one uses unrestricted HF and MP perturbation theory.

2. The energies of monomers, dimers, and the trimer, should be calculated with the same basis set of the whole trimer, a trimer centered basis set (TCBS)¹⁸.

3. In the case of trimers containing p-symmetry species, the monomer and dimer fragments should have the same orientation of the p-symmetry orbital as it is in the trimer. (The monomers have the orientation defined with respect to the ghost centers in TCBS.)

The first two conditions are well known and easily fulfilled. However, the third condition poses a problem as the orientation of the p-symmetry orbital in the trimer differs from that in the free dimers.

This paper is divided into two parts: the first deals with the H₃ and Na₃ trimers, and the second with the Na₂B trimer. The trimers were studied by the unrestricted Møller–Plesset (UMP*n*) perturbation theory within both the supermolecular and intermolecular perturbation frameworks. Including the hydrogen trimer in its quartet state is important because this trimer has served as a benchmark system for several decades, and serves as the simplest model for the treatment of the nonadditive interactions in van der Waals clusters^{22–27}.

The main part of this work is devoted to Na₂B which, compared with the other two trimers, exhibits a variety of novel features. First, calculations of the nonadditivity using the supermolecular approach are presented describing the following issues: the rotation of dimer potentials, the orientational nonadditivity, and the evaluation and analysis of the genuine nonadditivity. Next, perturbation calculations of the genuine nonadditivity are reported. The decomposition of first-order exchange energy is performed using the pseudodimer approach. The role and nature of three-body single-exchange (SE) and triple-exchange (TE) terms are analyzed and discussed.

For details and notation of the perturbation theory of the many-body effects and the pseudodimer approach, the reader is referred to our previous papers^{18,19,28,29}.

QUARTET STATE TRIMERS CONSISTING OF s-SYMMETRY MONOMERS

H_3 Trimer

The hydrogen trimer in its quartet state $^4A'_2$ has served as a benchmark system and the simplest model for the treatment of nonadditive interactions in van der Waals clusters²²⁻²⁷. To compare our results with previous theoretical studies, we performed some calculations for the triangle arrangements of Korona *et al.*²³ with their basis set. The calculations were performed for selected isosceles triangle arrangements of H_3 . The results were obtained with the aug-cc-pVTZ basis set of Dunning *et al.*³⁰⁻³², unless otherwise stated. The B126 basis set was used for comparison with ref.²³

The MP4 supermolecular and pseudodimer results are presented in Tables I and II, respectively. The partitioning of the Heitler–London exchange nonadditivity using the pseudodimer approach was proven to be robust enough for the equilateral-triangle rare gas trimers. Tables III and IV present a comparison with results of Korona *et al.*

The pairwise interaction energy as well as the whole interaction energy of the H_3 trimer are repulsive for all distances and levels of theory under consideration (see Table I). However, the correlation corrections to both the two-body and the whole interaction energy reduce the repulsion. In contrast to the pairwise energy, the three-body nonadditivity is attractive for all distances and levels of theory. The percentage value of the nonadditive energy amounts to about 20% of the total interaction energy for short-range distances.

The three-body nonadditivity is determined by the Heitler–London exchange nonadditivity (see Table II), with the leading TE term. The TE term is attractive for the triangle geometry and repulsive for the linear arrangements of H_3 . The SE term is of the opposite sign to that of the TE term. This behavior has also been observed for other trimers (*e.g.* rare gas trimers¹⁹).

The SE term and the SCF-deformation ($\Delta E_{\text{def}}^{\text{SCF}}$) term are of secondary importance. The SCF deformation exhibits a repulsive character for the smallest distances and angles. An interesting observation is that $\Delta E_{\text{def}}^{\text{SCF}}$ switches from attractive for $R > 3 \text{ \AA}$ to repulsive for $R < 3 \text{ \AA}$. This is in agreement with the previous findings for rare gas trimers⁵² as well as for the HCl and HF cyclic trimers⁵³. This suggests:

TABLE I

The supermolecular results for the interaction energy in the (${}^4A_2'$)H₃ trimer for the equilateral arrangement. Energy in μE_h

	<i>R</i> , Å	SCF	MP2	MP3	MP4(SDTQ)	%
$E_{\text{int}}(\text{total})$	0.8	493706.60	481262.16	478385.76	477579.29	
	1.4	112448.09	107169.21	105669.76	105158.05	
	2	25798.15	23840.03	23208.66	22976.73	
	2.6	5278.37	4548.01	4294.65	4198.33	
	3.4	518.76	325.43	252.95	224.28	
$E_{\text{int}}(\text{2-body})$	0.8	580266.36	568317.93	565210.92	564295.66	
	1.4	143029.07	137960.30	136449.85	135932.34	
	2	30912.54	28929.69	28279.13	28041.29	
	2.6	5881.40	5132.49	4870.02	4770.17	
	3.4	542.16	346.72	273.00	243.77	
$E_{\text{int}}(\text{3-body})$	0.8	-86559.76	-87055.77	-86825.16	-86716.37	-15.4
	1.4	-30580.98	30791.09	-30780.09	-30774.29	-22.6
	2	-5114.39	-5089.66	-5070.48	-5064.57	-18.1
	2.6	-603.03	-584.48	-575.36	-571.84	-12.0
	3.4	-23.40	-21.30	-20.05	-19.49	-8.0

TABLE II

The SE and TE contributions to the Heitler-London exchange nonadditivity for the equilateral arrangement of (${}^4A_2'$)H₃ trimer. The SE_part denotes partial SE term between only two H atoms, while the SE_tot denotes sum of all SE_part terms. Energy in μE_h

<i>R</i> , Å	SE_part	SE_tot	TE	$\epsilon_{\text{exch}}^{\text{HL}}$	$\Delta E^{\text{SCF}}[3,3]$	$\Delta E_{\text{def}}^{\text{SCF}}$
0.8	32999	98997	-333384	-234388	-86560	147828
1.4	5060	15179	-56663	-41484	-30581	10903
2	489.21	1467.62	-7277.05	-5809.43	-5114.39	695.04
2.6	35.61	106.82	-729.58	-622.76	-603.03	19.73
3	5.56	16.68	-140.08	-123.40	-124.60	-1.20
3.4	0.81	2.44	-24.97	-22.53	-23.40	-0.87

1. the same nature of $\Delta E_{\text{def}}^{\text{SCF}}$ in these complexes;
2. that there are at least two physically different mechanisms contributing to this correction, one prevailing at small R and the other at large R .

$\Delta E^{(2)}$ and $\Delta E^{(3)}$ are smaller by an order of magnitude than the SCF non-additivity for all distances (see Tables III and IV). One can also note that $\Delta E^{(3)}$ is smaller than the $\Delta E^{(2)}$ term for almost all distances. This trend is reversed at large distances (because $\Delta E^{(3)}$ includes the long-range three-body dispersion term, whereas $\Delta E^{(2)}$ vanishes exponentially).

A comment on the decomposition of the $\Delta E^{(2)}$ term should be made. The H_3 system has no intramonomer correlation effects and thus this term includes three components: the exchange-dispersion, the induction-dispersion, and the exchange-induction-dispersion¹⁸. The first two corrections have been calculated by Korona *et al.*²³ The exchange-dispersion, which is repulsive, prevails at large R and reasonably accounts for the whole second-order

TABLE III
Comparison of some three-body SAPT contributions calculated by Korona²³ with Heitler-London and supermolecular components for equilateral arrangement of the ($^4A_2'$) H_3 trimer for various interatomic distances. Energy in μE_h and interatomic distance in bohrs

$\theta = 60$	$R, \text{ \AA}$	4	6	7	8	10
Korona	$E_{\text{exch}}^{(1)}[3,3]$	-3832.0532	-58.9677	-5.8820	-0.5334	-0.0036
(B126)	$E_{\text{disp}}^{(3)}$	82.5326	3.7533	0.9609	0.2807	0.0349
	$E_{\text{ind-disp}}^{(2)}$	-252.4366	-3.4321	-0.3590	-0.0371	-0.0004
	$E_{\text{exch-disp}}^{(2)}$	119.8594	5.7741	1.0202	0.1567	0.0029
	$E_{\text{int}}[3,3]$	-3687.5043	-50.7339	-4.0653	-0.1160	0.0388
Present	SE_part	298.6851	2.3843	0.1792	0.0126	0.0001
(B126)	SE_tot	896.0552	7.1528	0.5375	0.0377	0.0002
	TE	-4728.1061	-66.1205	-6.4194	-0.5711	-0.0038
	$\epsilon_{\text{exch}}^{\text{HL}}$	-3832.0509	-58.9677	-5.8820	-0.5335	-0.0036
	$\Delta E_{\text{def}}^{\text{SCF}}$	382.3053	-1.4455	-0.3292	-0.0395	-0.0007
	$\Delta E^{(2)}$	29.0472	4.3117	0.7886	0.1192	0.0020
	$\Delta E^{(3)}$	17.9448	2.3856	0.5595	0.1326	0.0123
	$\Delta E^{(4)}$	5.7120	0.9768	0.2541	0.0699	0.0085
	MP4(SDTQ)	-3397.0416	-52.7390	-4.6090	-0.2513	0.0185

term. At small R , however, it appears (*cf.* Table III) that it is the induction-dispersion accompanied by exchange that dominates.

The total supermolecular and SAPT three-body energies of Korona *et al.*²³ agree remarkably well, although some small discrepancies are intriguing. A detailed comparison with the calculations of Korona *et al.* shows that the first-order exchange energies agree exactly. The second-order UMP three-body effect has a complex structure so it is not possible to compare it precisely with the SAPT energies. However, the third-order UMP energy is usually accurately reproduced by the third-order dispersion. This is not the case here, as even for $R = 8$ and 10 \AA , these terms markedly differ by a factor of two.

TABLE IV

Comparison of some SAPT nonadditive results with supermolecular and pseudodimer results for various isosceles geometries. Two H-H radii are fixed at $R = 6$ bohr and the angle between them is varied. Energy in μE_h

$R = 6$	Θ	30	60	90	120	150	180
Korona	$E_{\text{exch}}^{(1)}[3,3]$	-374.7375	-58.9651	-7.4002	-0.3419	0.8839	1.0975
(B81)	$E_{\text{disp}}^{(3)}$	16.7355	3.6059	0.9746	0.0517	-0.3072	-0.4029
	$E_{\text{ind-disp}}^{(2)}$	-20.3788	-3.2955	-0.6639	-0.2984	-0.2358	-0.2302
	$E_{\text{exch-disp}}^{(2)}$	33.8587	5.6679	1.6322	0.8020	0.6703	0.6672
	$E_{\text{int}}[3,3]$	-316.9620	-50.7872	-4.7160	0.6867	1.3820	1.4803
Present	SE_(H1..H2)	10.5560	2.3843	0.1820	-0.0784	-0.1211	-0.1285
(B126)	SE_(H1..H3)	10.5560	2.3843	0.1820	-0.0784	-0.1211	-0.1285
	SE_(H2..H3)	19.3464	2.3843	0.2426	0.0375	0.0113	0.0075
	SE_tot	40.4584	7.1528	0.6067	-0.1193	-0.2309	-0.2495
	TE	-415.2142	-66.1205	-8.0082	-0.2235	1.1140	1.3461
	$\epsilon_{\text{exch}}^{\text{HL}}$	-374.7558	-58.9677	-7.4015	-0.3428	0.8831	1.0966
	$\Delta E_{\text{def}}^{\text{SCF}}$	10.7840	-1.4455	-0.3017	0.2577	0.4919	0.5609
	$\Delta E^{(2)}$	19.0822	4.3117	1.2832	0.4219	0.1690	0.1181
	$\Delta E^{(3)}$	9.1699	2.3856	0.7804	0.2613	0.0899	0.0518
	$\Delta E^{(4)}$	3.5045	0.9768	0.3338	0.0855	-0.0118	-0.0371
	MP4(SDTQ)	-332.2152	-52.7390	-5.3059	0.6836	1.6221	1.7903

Na₃ Trimer

The supermolecular UMP n and IMPPT calculations were performed for the Na trimer in the high-spin $^4A'_2$ state. We essentially limited our study to the equilateral-triangle configuration, its side ranging from 2.5 to 7.6 Å. Some calculations were performed for two bonds fixed at 4.6 Å and for varied Θ angle between them, in order to expose the anisotropy of the nonadditive terms.

Table V collects the supermolecular results for the trimer, while Table VII provides a comparison of the supermolecular and perturbational energies.

TABLE V

The supermolecular two-body and three-body components of the total energy of the ($^4A'_2$)Na₃ trimer for the equilateral arrangement. Energy in μE_h

<i>R</i> , Å		3.6	4	4.4	4.6	4.8	5	5.2
<i>E</i> _{int}	SCF	11601.62	6574.60	3744.21	2873.61	2215.27	1711.78	1322.74
	MP2	5463.67	1125.13	-359.48	-693.3	-882.54	-975.5	-1003.51
	MP3	3020	-1002.8	-2037.99	-2171.06	-2180.15	-2112.58	-1998.07
<i>E</i> [2,3]	SCF	21939.88	11851.09	6497.84	4836.55	3608.75	2695.87	2013.49
	MP2	15550.2	6834.23	2562.23	1358.36	544.02	-7.03	-333.15
	MP3	13451.1	5002.35	1022.55	-35.01	-707.28	-1108.92	-1322.34
<i>E</i> [3,3]	SCF	-10338.26	-5375.49	-2753.63	-1962.94	-1393.48	-984.06	-690.75
	MP2	-10086.53	-5709.1	-2921.71	-2051.66	-1426.56	-982.53	-670.35
	MP3	-10431.1	-6005.15	-3060.54	-2136.05	-1472.87	1003.66	-675.73
<i>R</i> , Å		5.4	5.6	6	6.4	6.8	7.2	7.6
<i>E</i> _{int}	SCF	1019.86	783.13	453.85	255.73	139.88	74.23	38.25
	MP2	-988.25	-945.22	-816.12	-669.27	-529.66	-408.84	-310.48
	MP3	-1856.6	-1701.95	-1387.69	-1097.99	-849.41	-646.42	-486.79
<i>E</i> [2,3]	SCF	1501.52	1116.61	610.19	326.84	171.26	87.69	43.9
	MP2	-535.2	-641.97	-684.24	-614.23	-507.68	-400.47	-307.43
	MP3	-1407.33	-1407.21	-1266.51	-1051.83	-833.73	-642.21	-486.39
<i>E</i> [3,3]	SCF	-481.66	-333.48	-156.34	-71.11	-31.38	-13.47	-5.65
	MP2	-453.05	-303.25	-131.88	-55.03	-21.98	-8.38	-3.05
	MP3	-449.27	-294.74	-121.18	-46.16	-15.68	-4.21	-0.4

From the results of Table V one can tell that the van der Waals minimum of the Na₂ dimer at the UMP3 level of theory is located at 5.4 Å and is -469.11 μE_h deep, while the minimum of the trimer lies distinctly closer, at the distance equal to 4.8 Å, and the interaction energy amounts to -2180.15 μE_h. For the equilibrium geometry of Na₃, the two-body parts of the interaction energy amount to only 30%, while the rest is the three-body effect. The total nonadditivity is attractive for all distances under consideration, while two-body total effect is attractive for long distances and repulsive for short distances. This is in agreement with the findings of Higgins *et al.*¹¹, who had a better representation of the two-body potential (HF + dispersion model), and thus located the dimer and trimer minima at somewhat shorter distances. Indeed, our MP3 two-body energies are certainly not basis set saturated, and thus not attractive enough – the fourth-order terms would provide additional attraction.

To elucidate the origin of the extraordinarily large three-body forces, perturbation contributions are collected and plotted in Table VI and Fig. 2. The Heitler–London exchange, dispersion and SCF deformation are presented, and compared with the SCF, UMP2, UMP3 and correlation corrections.

TABLE VI

The (⁴A₂)Na₃ trimer. Comparison of perturbative results with the SCF deformation and supermolecular results. Energy in μE_h

<i>R</i> , Å	ε _{exch} ^{HL}	ε _{disp} ⁽³⁰⁾	ΔE _{def} ^{SCF}	ΔE ^{SCF}	E ^(MP2)	E ^(MP3)	ΔE ⁽²⁾	ΔE ⁽³⁾
4	-4305.37	341.22	-1070.12	-5375.49	-5709.10	-6005.15	-333.61	-296.05
4.2	-3313.47	260.01	-537.73	-3851.20	-4114.68	-4325.97	-263.47	-211.29
4.4	-2514.78	197.52	-238.85	-2753.63	-2921.71	-3060.54	-168.08	-138.83
4.6	-1882.81	149.66	-80.12	-1962.94	-2051.66	-2136.05	-88.72	-84.39
4.8	-1391.03	113.17	-2.45	-1393.48	-1426.56	-1472.87	-33.09	-46.31
5.2	-730.59	64.47	39.84	-690.75	-670.35	-675.73	20.40	-5.38
5.6	-365.70	36.69	32.22	-333.48	-303.25	-294.74	30.23	8.51
6	-175.22	20.95	18.88	-156.34	-131.88	-121.18	24.46	10.70
6.4	-80.68	12.05	9.57	-71.11	-55.03	-46.16	16.07	8.87
6.8	-35.83	6.99	4.45	-31.38	-21.98	-15.68	9.40	6.30
7.2	-15.41	4.11	1.94	-13.47	-8.38	-4.21	5.09	4.17
7.6	-6.43	2.46	0.78	-5.65	-3.05	-0.40	2.60	2.65

One can see in Fig. 2 that the nonadditivity of the Na_3 trimer is dominated by the Heitler–London exchange energy. In the minimum of Na_3 interaction energy (4.8 Å), the difference between the Heitler–London exchange energy and the SCF nonadditivity is less than $2.5 \mu E_h$. The gap be-

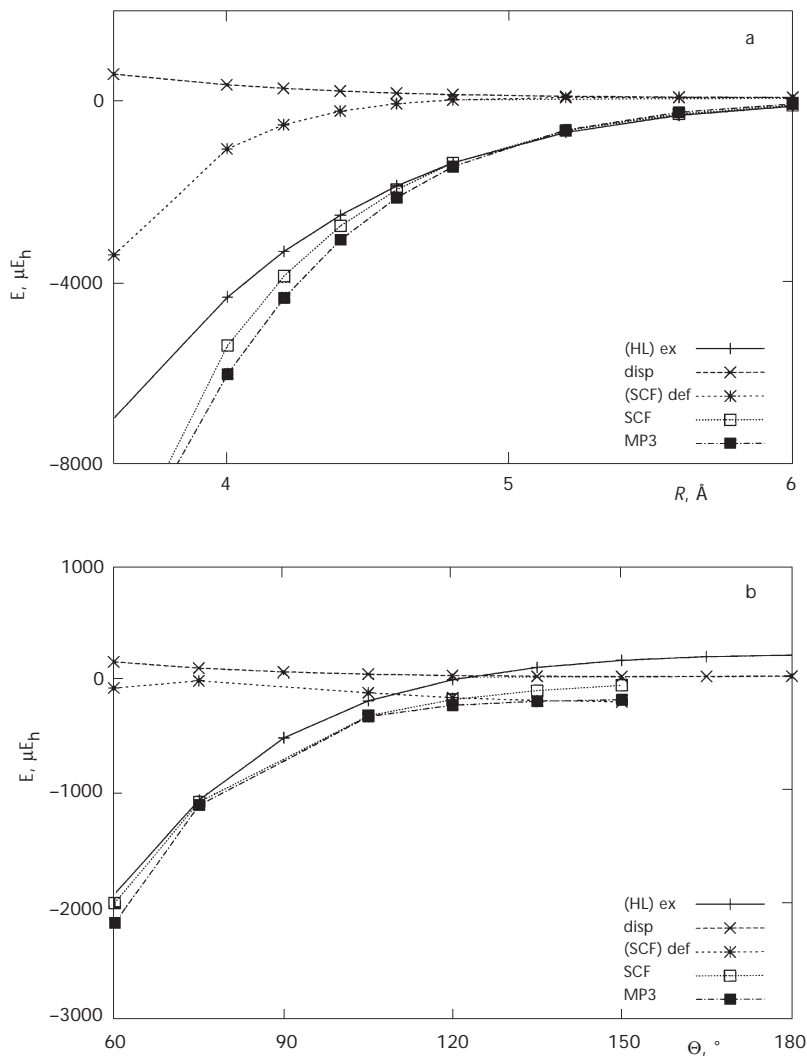


FIG. 2

The three-body terms in the Na_3 trimer from the IMPPT calculations. The labels: disp, ind, (HL)ex, SCF, (SCF)def denote: $\epsilon_{\text{disp}}^{(30)}$, $\epsilon_{\text{ind},r}^{(30)}$ [2(1),3(1)], Heitler–London exchange, SCF nonadditivity, and SCF deformation, respectively. $\Theta = 60^\circ$ (a), $R = 4.6$ Å (b)

tween the $\Delta E^{\text{SCF}}[3,3]$ and $\varepsilon_{\text{exch}}^{\text{HL}}$ is relatively small for longer distances, but it increases up to 30% for the shorter interatomic distances (at 3.6 Å). This gap defines the SCF-deformation nonadditivity $\Delta E_{\text{def}}^{\text{SCF}}$, and may be viewed as the nonadditive effect of the induction interaction modified by the accompanying exchange effects. Note that the effect changes its sign at around 4.8 Å, from attractive at smaller R to repulsive at larger R .

The correlation nonadditivities, included in $\Delta E^{(2)}$ and $\Delta E^{(3)}$, are of secondary importance, but not to be neglected quantitatively. Both are similar in magnitude and both change their signs in the van der Waals minimum region from minus at small R to plus at large R . At larger R , $\Delta E^{(3)}$ agrees well with the dispersion nonadditivity, and at smaller R it is apparently affected strongly by the exchange and charge-overlap effects. Interestingly, the purely exchange nonadditivity of $\Delta E^{(2)}$ is as important as $\Delta E^{(3)}$.

To better understand the nature of the exchange effect, the SE and TE terms of Heitler–London exchange energy are plotted in Fig. 3 and compared with the SCF energy as a function of the interatomic distance for the equi-

TABLE VII

The SE and TE components of the Heitler–London exchange nonadditivity in the (${}^4\text{A}_2$) Na_3 trimer calculated *via* pseudodimer approach in comparison to the SCF deformation. Energy in μE_{h}

R , Å	SE_part	SE_tot	TE	$\varepsilon_{\text{exch}}^{\text{HL}}$	ΔE^{SCF}
3.2	7035.61	21106.82	-31692.69	-10585.87	-
3.6	3502.45	10507.36	-17466.55	-6959.19	-10338.26
4	1661.37	4984.12	-9289.48	-4305.37	-5375.49
4.2	1125.77	3377.32	-6690.79	-3313.47	-3851.20
4.4	755.18	2265.55	-4780.33	-2514.78	-2753.63
4.6	501.77	1505.31	-3388.12	-1882.81	-1962.94
4.8	330.40	991.20	-2382.23	-1391.03	-1393.48
5.2	139.66	418.99	-1149.58	-730.59	-690.75
5.6	57.15	171.46	-537.17	-365.70	-333.48
6	22.67	68.00	-243.22	-175.22	-156.34
6.4	8.73	26.18	-106.86	-80.68	-71.11
6.8	3.27	9.80	-45.63	-35.83	-31.38
7.2	1.19	3.58	-18.98	-15.41	-13.47
7.6	0.42	1.27	-7.71	-6.43	-5.65

lateral-triangle geometry. All the results are collected in Table VII. The SE term represents the coupling between the exchange of two electrons originating from two monomers with the electrostatic interaction with the third monomer. There are three possibilities of such coupling, which differ in various permutation of the monomers. In the case of the equilateral trian-

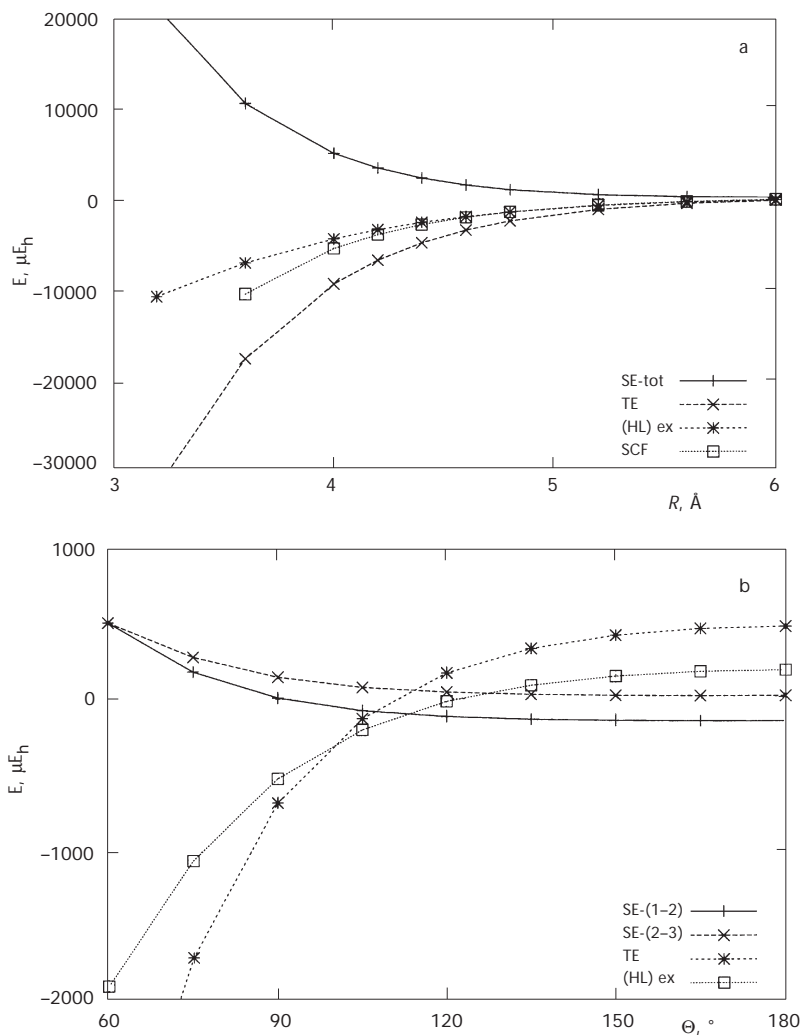


FIG. 3

The SE and TE exchange contributions to the Heitler-London exchange energy compared with the SCF nonadditivity in the Na_3 system. The R dependence is shown for the equilateral triangle ($\Theta = 60^\circ$) (a), and the angular dependence for the NaB distances fixed at 4.6 \AA value (b)

gle, all three SE parts are equal. As a consequence, the total SE term, which is denoted here as SE_tot, is the SE term multiplied by 3.

The TE term represents the part of the exchange nonadditivity involving the exchange of electrons from all three monomers, coupled with electrostatic interaction. In the case of Na₃ for studied geometries, the attractive character of the Heitler–London energy is determined by the triple exchange term. On the other hand, the SE term, which exhibits the opposite behavior, cannot be neglected. The balance between SE and TE terms creates the specific anisotropy of the Heitler–London exchange energy and can cause dramatic changes in the interaction energy from attractive to repulsive.

The angular dependence of the nonadditivity in the Na₃ cluster was also evaluated for the isosceles-triangle geometry. Distances between atoms Na(1)–Na(2) and Na(1)–Na(3) were fixed at 4.6 Å, the distance related to the minimum energy especially of the Na₃ cluster. The angle Na(2)–Na(1)–Na(3) was varied from 60 to 180° with the step of 15°. The results are presented in Table VIII.

Table VIII shows different interaction energy contributions. The angular dependence of nonadditivity shows that the Heitler–London exchange effects are large and important for all Θ , whereas the importance of the SCF

TABLE VIII

Angular dependence of various three-body components of the interaction energy of the (⁴A₂)Na₃ trimer. The interatomic distance was fixed at 4.6 Å. The number in parentheses labels Na atoms from which electrons are exchanged. The Θ angle Na(2)–Na(1)–Na(3) is varied. Energy in μE_h

Θ	SE_(1-2)	SE_(2-3)	SE_tot	TE	$\epsilon_{\text{exch}}^{\text{HL}}$	$\Delta E_{\text{def}}^{\text{SCF}}$	$\epsilon_{\text{disp}}^{(30)}$	ΔE^{SCF}
60	501.77	501.77	1505.31	-3388.12	-1882.81	-80.12	149.66	-1962.94
75	179.98	276.29	636.24	-1683.81	-1057.57	-18.99	92.79	-1076.56
90	8.09	144.80	160.98	-681.05	-520.07		57.20	
105	-74.90	76.88	-72.91	-127.28	-200.19	-129.68	34.29	-329.87
120	-114.63	43.41	-185.86	169.37	-16.49	-175.34	19.54	-191.83
135	-134.03	26.98	-241.09	328.71	87.62	-203.55	10.19	-115.93
150	-143.52	18.90	-268.13	413.45	145.32	-218.45	4.50	-73.132
165	-147.81	15.16	-280.45	454.79	174.34		1.43	
180	-149.02	14.07	-238.98	467.15	183.17		0.46	

deformation grows with the increasing angle. For angles larger than 120° , the value of the SCF deformation is similar to the total supermolecular MP3 nonadditivity.

The $\varepsilon_{\text{exch}}^{\text{HL}}$ term shows a strong anisotropy determined mainly by the TE term (see Fig. 3). The change of sign of $\varepsilon_{\text{exch}}^{\text{HL}}$, as well as TE and SE_(1-2), is observed at about 100° (see Fig. 3). For small angles the Heitler-London exchange energy shows a negative sign while for larger angles it is positive.

The dispersion nonadditive term is relatively small for all Θ . It barely influences the total nonadditivity.

To summarize, the geometry and energetics of the Na_3 cluster is determined by the two-body potential of the Na_2 dimer and attractive three-body exchange effects. The three-body nonadditive energy amounts to 65% of the total interaction energy at the UMP3 level of theory. For all studied distances, the whole nonadditivity is attractive and considerably shortens the interatomic trimer equilibrium distance with respect to the Na_2 dimer equilibrium distance. The minimum energy of the Na_2 dimer is located at 5.4 \AA while that of the Na_3 trimer at 4.8 \AA . The three-body energy is dominated by the Heitler-London exchange energy and especially by its TE component. It originates from the Pauli exclusion principle imposed on the unperturbed monomers; a serious net reduction of the exchange effect is observed after attaching a third monomer. The three-body induction and dispersion effects are of secondary importance.

THE LOWEST QUARTET STATES OF THE Na_2B TRIMER

The isosceles-triangle arrangement of the Na_2B trimer was assumed in all calculations. Three quartet states of the Na_2B trimer were studied, derived from the $2s_{\text{B}}^2 2p_{\text{B}}^1 3s_{\text{Na1}}^1 3s_{\text{Na2}}^1$ electronic configuration, and related to the A_2 , B_2 , and A_1 symmetries. For the isosceles-triangle arrangements, the singly occupied $3s$ orbitals of Na atoms form an orbital of the a_1 and b_2 symmetry of the trimer. The singly occupied p orbital of boron is the source of the variety states in Na_2B . The A_2 state occurs when the singly occupied p orbital is perpendicular to the Na-B-Na plane (b_1 symmetry). The B_2 state occurs when the singly occupied p orbital of B atom is located in the Na-B-Na plane and is perpendicular to the Na-Na dimer axis (a_1 symmetry). The A_1 symmetry occurs when the p orbital lies in the plane Na-B-Na, but is parallel to the Na-Na dimer axis (b_2 symmetry). For other geometries, C_{2v} is reduced to the C_s symmetry. In such a case, the B_1 state becomes the A'' state, whereas the A_1 and B_2 states give rise to two A' states. For the collinear ar-

rament Na-B-Na, the B_2 state transforms into the Σ state whereas the A_1 and B_1 states degenerate to form the Π state.

Hereafter, the labels of p orbital symmetry in the trimer will be used to describe different states of Na_2B in the text. Such a convention ensures transparent notation consistent with the $RG_2B(^2P)$ type of complex.

The supermolecular method through the UMP3(full) level of theory, IMPPT and pseudodimer approaches were applied^{33,34}. In addition, the NaB dimer was studied at the UMP4 level of theory. All calculations were performed with the aug-cc-pVTZ basis set for B, and Gutowski's basis set for Na¹⁰.

To obtain supermolecular pairwise and nonadditive energy in the Na_2B , monomers and dimers should have the same orientation of the p-symmetry orbital as it is in the trimer. More specifically, if the monomer, dimer and trimer calculations are performed with the TCBS, one obtains the monomers and trimer having the orientation and symmetry shown in Fig. 1, but the dimer comes out within the Σ and Π symmetries as in Fig. 4. The orientations of the p orbital in monomers coincides with that of the trimer, due to the same symmetry of Hamiltonian within TCBS.

In the case of the A_1 and B_2 states, the direction of the p orbital is rotated by $\Theta/2$ or $(\pi/2 - \Theta/2)$ with respect to the Π and Σ states of the NaB dimer, where Θ is the angle between two Na-B bonds. In order to have consistent alignment of the p orbital in the monomer and dimers, the dimers should be first rotated to the same orientation as in the trimer, that is, from the Σ and Π dimer adiabatic states to the A_1 and B_2 diabatic dimer states. Hereafter we call the energetic effect of this transformation the *orientational nonadditivity*. In the literature³⁵⁻³⁷ one may also find the term "matrix

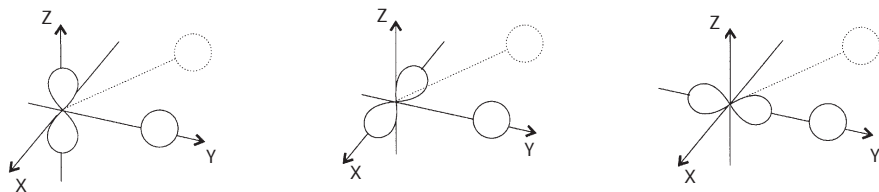


FIG. 4

Orientation of the p orbital in the NaB dimer within TCBS frame of Na_2B is determined with respect to the Na atom, but also with respect to the ghost atom. The B and Na atoms are drawn with solid lines while the ghost atom is drawn with a dotted line. The solution of the Schrödinger equation gives two Π states and one Σ . The ghost removes the degeneracy of the Π state. One Π state is coplanar with the Na_2B plane while the other is perpendicular. The figures show the NaB dimer in Π -perpendicular, Π -coplanar, and Σ -coplanar states, respectively

nonadditivity". It is the change of the pair interaction energy of Na and B in the cluster caused by the reorientation of the open-shell orbital from the Π and Σ states, due to the appearance of the third monomer.

Once the orientation of the p orbital in the trimer, dimers and monomers is the same, then Eqs (2)–(5) yield the nonadditive effect that we hereafter refer to as the *genuine three-body nonadditivity*. It may be further dissected into the exchange, induction, dispersion, *etc.* nonadditivities^{18,19}.

Nonadditivity from Supermolecular Approach

Rotation of Two-Body Interaction Potentials

The orientation of the singly occupied p orbital in the TCBS calculations^{18,19,28} of monomers is the same as in the trimer for both the A_1 and B_2 states. However, calculations of the NaB dimer with TCBS provide states of the $C_{\infty v}$ symmetry: one Σ state and two Π states. Two instead of one Π states arise because of TCBS which fixes the Na_2B plane in space and distinguishes between the coplanar (with the TCBS plane) Π state and perpendicular (to the TCBS plane) Π state. Let us denote the related interactions as V_{Π}^{copl} and V_{Π}^{perp} , respectively.

In order to obtain the C_{2v} symmetry dimers, one should rotate the coplanar energies of the NaB dimers. In general, the interaction of two species, one of the spherical symmetry as the Na atom and one of the p symmetry as the B atom, could be expanded in terms of the isotropic part and the anisotropy of the interaction^{38–41}

$$V(R, \vartheta) = V_0(R) + P_2(\cos \vartheta) \cdot V_2(R), \quad (6)$$

where V_0 , V_2 , and P_2 denote, respectively, the isotropic interaction, the anisotropy of interaction, and the Legendre polynomial of the second order. The above Eq. (6) extrapolates the Π and Σ states, which correspond respectively to $\cos \vartheta$ equal to 0 and 1, to any arbitrary orientations.

Averaging over all possible states of NaB dimer gives the value of the isotropic term:

$$V_0 = \frac{1}{3}(2V_{\Pi} + V_{\Sigma}). \quad (7)$$

The anisotropic part of interaction is

$$V_2 = \frac{5}{3}(V_\Sigma - V_\Pi). \quad (8)$$

Using the explicit expressions of the V_0 and V_2 components in terms of V_Σ and V_Π , the orientational dependence of interaction between the s-symmetry and p-symmetry orbitals amounts to:

$$V(R, \vartheta) = V_\Pi(R) + (V_\Sigma(R) - V_\Pi(R)) \cdot \cos^2 \vartheta, \quad (9)$$

where ϑ is the angle between the p orbital and the bond axis. The angular dependence of the interaction potential from the Legendre expansion is shown in Fig. 5.

In the case of the Na_2B trimer, it is more convenient to express the interaction energies for the A_1 and B_2 states of both NaB dimers by the angle Θ instead of the angle ϑ . The Θ angle is measured between the two NaB bonds; for the A_1 and B_2 states of the isosceles Na_2B arrangement, it strictly relates to ϑ . In the case of the A_1 state, half of Θ is equal to the ϑ angle, and in the case of the B_2 state the ϑ angle complements the right angle:

$$\vartheta_{A_1} = \frac{1}{2}\Theta \quad (10)$$

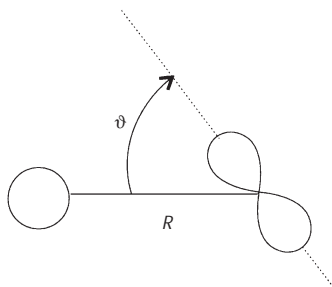


FIG. 5

According to the Legendre expansion, the interaction potential of the NaB dimer may be expressed as a simple function of the isotropic potential V_0 and the anisotropic part V_2 for any orientation of the p orbital: $V(R, \vartheta) = V_0(R) + V_2(R) \cdot P_2(\cos \vartheta)$

$$\vartheta_{B_2} = \frac{1}{2}\pi - \frac{1}{2}\Theta. \quad (11)$$

Relationships between angles ϑ_{A_1} , ϑ_{B_2} , and Θ in isosceles trimers are explicitly showed in Fig. 6. Applying these relationships to the NaB dimer with the trimer-centered basis of the Na_2B system in isosceles geometry gives energies of the dimers with the reoriented p orbital. For example, the interaction energy of the NaB dimer in the A_1 and B_2 arrangements is given by ref.³⁹

$$V_{A_1} = V_{\Sigma} \cos^2(\Theta/2) + V_{\Pi} \sin^2(\Theta/2) \quad (12)$$

$$V_{B_2} = V_{\Sigma} \sin^2(\Theta/2) + V_{\Pi} \cos^2(\Theta/2), \quad (13)$$

where the Θ angle is the Na-B-Na angle. For the sake of the consistency of the numerical procedure, the V_{Σ} and V_{Π} terms are coplanar, V_{Σ}^{copl} and V_{Π}^{copl} , in the above equations. Similarly the B_1 state is a pure V_{Π}^{perp} perpendicular state.

We are now in a position to write down the total energies of the dimers properly “reoriented”:

$$E_{\text{tot}}^{A_1}(\text{NaB}) = E_{\text{tot}}^{\Sigma, \text{copl}}(\text{NaB}) \cdot \cos^2(\Theta/2) + E_{\text{tot}}^{\Pi, \text{copl}}(\text{NaB}) \cdot \sin^2(\Theta/2) \quad (14)$$

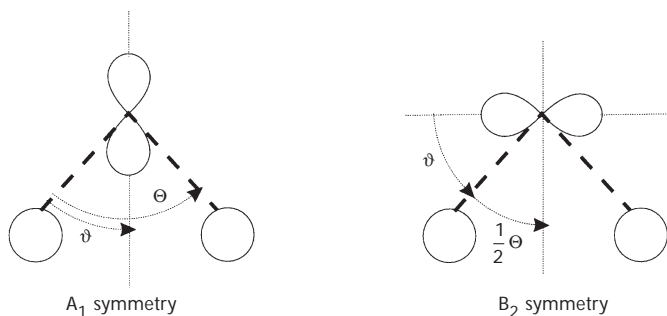


FIG. 6

In the isosceles arrangement of the Na_2B trimer the orientation of the p orbital of the B atom is symmetric, so angle ϑ between the B-Na axis and the p orbital may be simply expressed in terms of the Na-B-Na Θ angle. The A_1 state corresponds to $\vartheta = \Theta/2$ while in the case of B_1 one has $\vartheta = \pi/2 - \Theta/2$

$$E_{\text{tot}}^{\text{B}_1}(\text{NaB}) = E_{\text{tot}}^{\Pi, \text{perp}}(\text{NaB}) \quad (15)$$

$$E_{\text{tot}}^{\text{B}_2}(\text{NaB}) = E_{\text{tot}}^{\Sigma, \text{copl}}(\text{NaB}) \cdot \sin^2(\Theta/2) + E_{\text{tot}}^{\Pi, \text{copl}}(\text{NaB}) \cdot \cos^2(\Theta/2). \quad (16)$$

These energies may be readily used in Eqs (2)–(5) to obtain genuine three-body nonadditivity. It is also of interest to derive the related two-body interaction energies in the A_1 and B_2 orientations of the p orbital

$$V_{A_1} = E_{\text{tot}}^{A_1}(\text{NaB}) - E_{\text{tot}}^{A_1}(\text{B}) - E_{\text{tot}}(\text{Na}) \quad (17)$$

$$V_{B_1} = E_{\text{tot}}^{\text{B}_1}(\text{NaB}) - E_{\text{tot}}^{\text{B}_1}(\text{B}) - E_{\text{tot}}(\text{Na}) \quad (18)$$

$$V_{B_2} = E_{\text{tot}}^{\text{B}_2}(\text{NaB}) - E_{\text{tot}}^{\text{B}_2}(\text{B}) - E_{\text{tot}}(\text{Na}). \quad (19)$$

The values of the V_{Σ}^{copl} , V_{Π}^{copl} , and V_{Π}^{perp} interaction energies of the NaB dimer are collected in Table IX. The first and the second sections describe, respectively, the coplanar Π and Σ interactions of NaB obtained by the rotation of the p orbital of the B atom from the A_1 and B_2 symmetries. The last section describes the perpendicular Π interaction of NaB obtained from the B_1 symmetry of the B atom and NaB dimer.

The Orientational Nonadditivity

The most appropriate definition of the two-body orientation nonadditivity is with respect to the isotropic part of the potential V_0 . The reference levels are introduced separately for each NaB pair (*cf.* ref.³⁹). Moreover, it is convenient to introduce two reference energy levels for each NaB pair. One of them is the coplanar isotropic potential V_0^{copl} , and the other is the perpendicular isotropic potential V_0^{perp} . These potentials were obtained as averages over the well separated states of the NaB dimer in the Na_2B trimer. For any arrangement of the Na_2B trimer, the A'' (or B_1) state is well separated from the others with the perpendicular p orbital of B (the V_{Π}^{perp} potential). Similarly, both A_0 states (or A_1 and B_2) are combinations of two coplanar

states (V_{Π}^{copl} and V_{Σ}^{copl}). The V_0^{perp} isotropic perpendicular potential is equal to V_{Π}^{perp} , while the coplanar isotropic one V_0^{copl} is equal to $\frac{1}{2}(V_{\Sigma}^{\text{copl}} + V_{\Pi}^{\text{copl}})$.

The total orientational nonadditivities in the A_1 , B_1 , and B_2 states are the sums of contributions of nonadditivities from pair interactions Na(1)–B and Na(2)–B:

$$V_{\text{NON}}^{\text{copl},A_1} = V_{\text{NON}}^{\text{copl},A_1}(\text{Na(1)B}) + V_{\text{NON}}^{\text{copl},A_1}(\text{Na(2)B}) \quad (20)$$

$$V_{\text{NON}}^{\text{copl},B_2} = V_{\text{NON}}^{\text{copl},B_2}(\text{Na(1)B}) + V_{\text{NON}}^{\text{copl},B_2}(\text{Na(2)B}) \quad (21)$$

$$V_{\text{NON}}^{\text{perp},B_1} = V_{\text{NON}}^{\text{perp},B_1}(\text{Na(1)B}) + V_{\text{NON}}^{\text{perp},B_1}(\text{Na(2)B}). \quad (22)$$

TABLE IX

Interaction energies of the NaB dimer with properly oriented monomers as in the Σ and Π states of the dimer. Energy in μE_h

$R, \text{ \AA}$	V_{Π}^{copl}			V_{Σ}^{copl}			V_{Π}^{perp}		
	SCF	MP2	MP3	SCF	MP2	MP3	SCF	MP2	MP3
4	-414.81	-2795.27	-3204.47	2129.34	1318.47	1118.79	-413.67	-2792.98	-3201.65
4.2	-247.19	-2098.37	-2428.79	1663.53	923.86	739.92	-246.51	-2096.84	-2426.64
4.4	-150.48	-1590.18	-1856.04	1279.03	619.63	453.52	-150.08	-1589.19	-1854.39
4.6	-94.32	-1212.54	-1425.75	967.99	391.46	243.89	-94.04	-1211.91	-1424.49
4.8	-61.13	-928.93	-1099.59	721.64	225.59	96.18	-60.92	-928.55	-1098.64
5	-41.01	-714.67	-851.23	530.43	109.11	-3.16	-40.81	-714.43	-850.51
5.2	-28.43	-552.20	-649.03	384.72	30.51	-61.86	-28.25	-552.08	-661.05
5.4	-20.28	-428.62	-516.38	275.55	-19.93	-102.42	-20.08	-428.53	-515.98
5.6	-14.84	-334.30	-404.92	194.98	-50.13	-120.22	-14.60	-334.23	-404.60
6	-8.42	-206.49	-252.65	94.10	-72.73	-122.77	-8.13	-206.48	-252.52
6.4	-5.04	-130.37	-161.00	43.12	-69.84	-105.26	-4.74	-130.36	-160.93
6.8	-3.08	-84.19	-104.85	18.56	-58.18	-83.21	-2.86	-84.23	-104.88
7.2	-1.95	-55.74	-69.94	7.30	-45.36	-63.09	-1.74	-55.74	-69.93
7.6	-1.25	-37.85	-47.78	2.38	-34.24	-46.90	-1.10	-37.84	-47.77

The orientational nonadditivity of the Na(1)B and Na(2)B interactions is defined as the difference between the interaction energy of the dimer with the p orbital rotated by ϑ_1 and ϑ_2 (as in Fig. 1) from the respective NaB bonds:

$$V_{\text{NON}}^{\text{X,Y}}(\text{Na}(i)\text{B}) = V^{\text{X,Y}}(R_i, \vartheta_i) - V_0^{\text{X}}(\text{Na}(i)\text{B}), \quad (23)$$

where $i = 1, 2$ and $X = \text{copl}, \text{perp}$. Y stands for A_1 or B_2 for $X = \text{copl}$ and B_1 for $Y = \text{perp}$. The last equation gives zero as the orientational nonadditivity for the B_1 state. The following simple expressions are obtained for the isosceles-triangle arrangements of Na_2B

$$V_{\text{NON}}^{\text{copl},A_1} = +\cos\Theta \cdot (V_{\Sigma}^{\text{copl}} - V_{\Pi}^{\text{copl}}), \quad (24)$$

$$V_{\text{NON}}^{\text{copl},B_2} = -\cos\Theta \cdot (V_{\Sigma}^{\text{copl}} - V_{\Pi}^{\text{copl}}), \quad (25)$$

where the angle Θ is measured between the two interatomic NaB axes in the Na_2B triangle. A detailed derivation has been given in ref.⁴²

Since in our case all calculations were performed for the equilateral geometries of the Na_2B trimer, one can easily show that the orientational nonadditivity is explicitly given by:

$$V_{\text{NON}}^{\text{copl},A_1} = +\frac{1}{2} V_{\Sigma}^{\text{copl}} - \frac{1}{2} V_{\Pi}^{\text{copl}} \quad (26)$$

$$V_{\text{NON}}^{\text{copl},B_2} = -\frac{1}{2} V_{\Sigma}^{\text{copl}} + \frac{1}{2} V_{\Pi}^{\text{copl}}. \quad (27)$$

The values of the orientational nonadditivity of the Na_2B system for the A_1 and B_2 states are collected in Table X. A comparison of the orientational vs genuine nonadditivities with the isotropic part of the interaction is shown in Fig. 7.

The orientational nonadditivity for the A_1 state has the same value as for the B_2 state, but of the opposite sign. The formulas for the nonadditivity (Eqs (24)–(25)) show that it vanishes when V_{Σ} is equal to V_{Π} . This is intu-

tively reasonable. Additionally, the nonadditivity vanishes when Θ is the right angle. This is because for the right angle both the NaB potentials are exactly equal to the values of the reference isotropic potential.

One can see in Table XI that from the energetic point of view it is advantageous to turn into the B_2 direction and not advantageous to turn into the A_1 direction. The magnitude of the orientational nonadditivity is comparable with the total isotropic V_0^{copl} pairwise interaction energy of the NaB dimer. This is because the B_2 state is closer to the Π state and the A_1 to the Σ state.

BSSE and Its Orientational Dependence

The isotropic p-orbital orientation-independent BSSE occurs in the B_1 state. Its values were obtained by subtraction of the TCBS energy of the B_1 symmetry B atom and the MCBS energy of the B atom.

TABLE X

The interaction energy of the NaB dimer obtained within TCBS framework for the equilateral-triangle arrangement of Na_2B . The orientation of the singly occupied p orbital of the B atom is the same as in A_1 , B_2 , and B_1 symmetries of the quartet state of the Na_2B trimer. Energy in μE_h

$R, \text{\AA}$	A_1			B_2			B_1		
	SCF	MP2	MP3	SCF	MP2	MP3	SCF	MP2	MP3
4	1494.25	296.55	44.31	220.28	-1773.35	-2129.99	-413.67	-2792.98	-3201.65
4.2	1187.24	175.29	-45.12	229.10	-1349.80	-1643.75	-246.51	-2096.84	-2426.64
4.4	923.39	74.50	-116.31	205.15	-1045.05	-1286.39	-150.08	-1589.19	-1854.39
4.6	704.41	-2.13	-165.50	169.26	-818.95	-1016.36	-94.04	-1211.91	-1424.49
4.8	528.08	-55.86	-194.89	132.43	-647.48	-808.52	-60.92	-928.55	-1089.64
5	389.65	-90.22	-207.90	99.77	-515.33	-646.48	-40.81	-714.43	-850.51
5.2	283.24	-109.45	-208.66	73.06	-412.24	-502.23	-28.25	-552.08	-661.05
5.4	202.94	-117.48	-200.88	52.33	-331.07	-417.92	-20.08	-428.53	-515.98
5.6	143.34	-117.68	-187.65	36.80	-266.75	-337.49	-14.60	-334.23	-404.60
6	68.42	-104.50	-153.53	17.27	-174.72	-221.88	-8.13	-206.48	-252.52
6.4	30.77	-84.18	-118.44	7.31	-116.03	-147.81	-4.74	-130.36	-160.93
6.8	13.01	-64.11	-88.07	2.47	-78.27	-99.98	-2.86	-84.23	-104.88
7.2	5.05	-47.41	-64.26	0.30	-53.69	-68.77	-1.74	-55.74	-69.93
7.6	1.60	-34.69	-46.64	-0.47	-37.40	-48.03	-1.10	-37.84	-47.77

Table XII lists the values of BSSE for the B1 state in comparison with the values of the total interaction energy for this state. One can see that BSSE is over one order of magnitude larger at the correlated levels of theory than at the SCF level, at any interatomic distances.

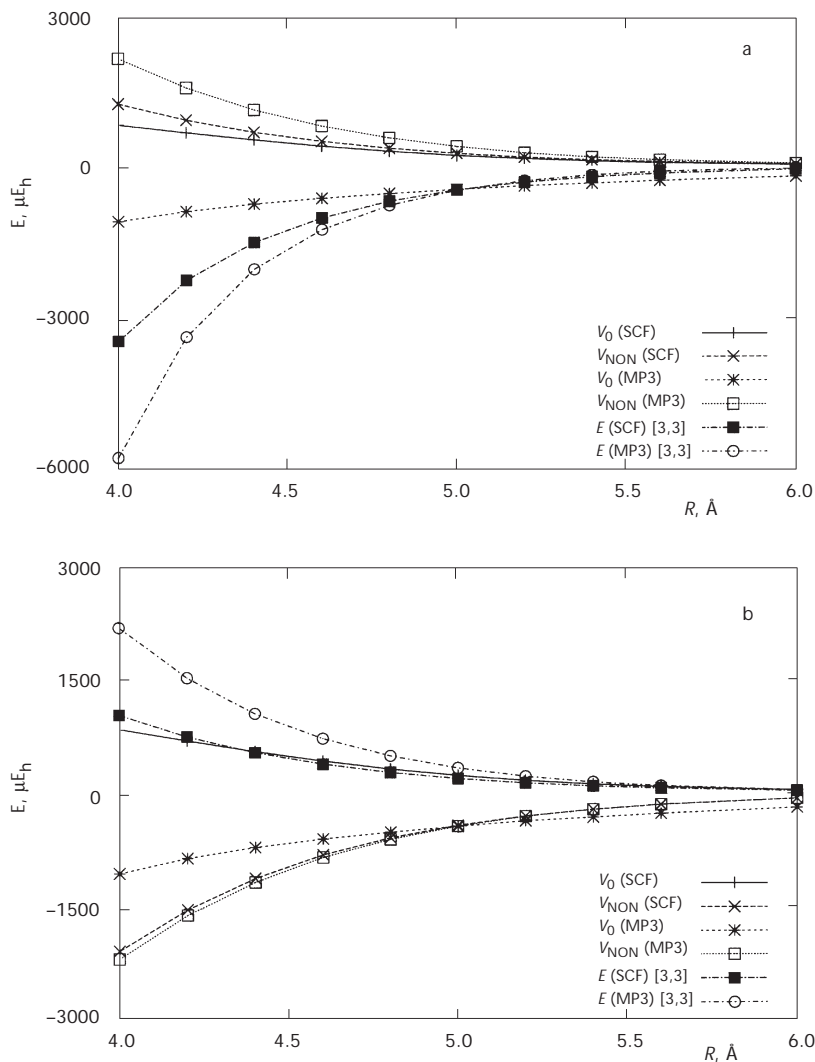


FIG. 7

Comparison between the orientational and genuine parts of the nonadditivity in Na_2B at the SCF and MP3 levels of theory. V_0 , V_{NON} , and E [3,3] denote, respectively, isotropic interaction, orientational, and genuine nonadditivity. A_1 state, $\Theta = 60^\circ$ (a); B_2 state, $\Theta = 60^\circ$ (b)

To clarify the idea of the orientational dependence of BSSE, one may consider the difference between the “coplanar” and the “perpendicular” interaction energies of the Π state of the NaB dimer.

We also show in Table XIII the percentage values of BSSE in the A_1 and B_2 states. The percentage errors were calculated with respect to the Π perpendicular interaction of NaB:

$$\Delta(\Pi) = 100 \cdot (V_{\Pi}^{\text{copl}} - V_{\Pi}^{\text{perp}}) / V_{\Pi}^{\text{perp}} \quad (28)$$

$$\Delta(\text{BSSE} - A_1) = 100 \cdot (V_{\Pi}^{\text{copl}}(\text{BSSE} - A_1) - V_{\Pi}^{\text{perp}}) / V_{\Pi}^{\text{perp}} \quad (29)$$

$$\Delta(\text{BSSE} - B_2) = 100 \cdot (V_{\Pi}^{\text{copl}}(\text{BSSE} - B_2) - V_{\Pi}^{\text{perp}}) / V_{\Pi}^{\text{perp}}, \quad (30)$$

TABLE XI
Orientational nonadditivity of the Na_2B system for the A_1 and B_2 states. Energy in μE_h

$R, \text{\AA}$	SCF			MP2			MP3		
	V_0	$V_{\text{NON}}^{A_1}$	$V_{\text{NON}}^{B_2}$	V_0	$V_{\text{NON}}^{A_1}$	$V_{\text{NON}}^{B_2}$	V_0	$V_{\text{NON}}^{A_1}$	$V_{\text{NON}}^{B_2}$
4	857.26	1272.07	-1272.07	-738.40	2056.87	-2056.87	-1042.84	2161.63	-2161.63
4.2	708.17	955.36	-955.36	-587.25	1511.11	-1511.11	-844.44	1584.35	-1584.35
4.4	564.27	714.76	-714.76	-485.27	1104.90	-1104.90	-701.26	1154.78	-1154.78
4.6	436.84	531.15	-531.15	-410.54	802.00	-802.00	-590.93	834.82	-834.82
4.8	330.26	391.39	-391.39	-351.67	577.26	-577.26	-501.70	597.88	-597.88
5	244.71	285.72	-285.72	-302.78	411.89	-411.89	-427.19	424.04	-424.04
5.2	178.15	206.57	-206.57	-260.85	291.36	-291.36	-355.44	293.58	-293.58
5.4	127.63	147.92	-147.92	-224.27	204.34	-204.34	-309.40	206.98	-206.98
5.6	90.07	104.91	-104.91	-192.21	142.09	-142.09	-262.57	142.35	-142.35
6	42.84	51.26	-51.26	-139.61	66.88	-66.88	-187.71	64.94	-64.94
6.4	19.04	24.08	-24.08	-100.10	30.26	-30.26	-133.13	27.87	-27.87
6.8	7.74	10.82	-10.82	-71.19	13.00	-13.00	-94.03	10.82	-10.82
7.2	2.67	4.62	-4.62	-50.55	5.19	-5.19	-66.51	3.42	-3.42
7.6	0.56	1.82	-1.82	-36.05	1.81	-1.81	-47.34	0.44	-0.44

where BSSE- A_1 and BSSE- B_2 stand for the interaction calculated with the nonrotated B monomer in the A_1 and B_2 states, respectively.

$$V_{\Pi}^{\text{copl}}(\text{BSSE} - A_1) = E_{\text{tot}}^{\Pi, \text{copl}}(\text{NaB}) - E_{\text{tot}}^{A_1}(\text{B}) - E_{\text{tot}}(\text{Na}) \quad (31)$$

$$V_{\Pi}^{\text{copl}}(\text{BSSE} - B_2) = E_{\text{tot}}^{\Pi, \text{copl}}(\text{NaB}) - E_{\text{tot}}^{B_2}(\text{B}) - E_{\text{tot}}(\text{Na}) \quad (32)$$

It is clear from Table XIII that the orientational parts of BSSE are relatively small but not negligible. The reorientation of the open-shell monomer or dimers gives the lowest BSSE and is the appropriate procedure to obtain interaction energy with the smallest possible error.

TABLE XII

Basis set superposition error for the B_1 state of the Na_2B system in comparison with the three-body interaction energy for the same state. Energies in μE_h

$R, \text{\AA}$	BSSE			$E[3,3]$		
	SCF	UMP2	UMP3	SCF	UMP2	UMP3
4	-21.4	-754.6	-774.0	-1285.26	-1409.10	-1387.42
4.2	-19.1	-652.9	-667.8	-837.69	-795.30	-760.07
4.4	-16.9	-563.3	-574.7	-539.21	-441.49	-405.28
4.6	-15.0	-485.9	-494.8	-341.91	-238.71	-206.70
4.8	-13.2	-421.4	-429.3	-213.35	-124.39	-98.16
5	-11.7	-370.0	-377.9	-130.94	-61.51	-40.95
5.2	-10.6	-330.3	-339.1	-78.97	-28.02	-12.40
5.4	-9.9	-299.9	-310.0	-46.79	-11.02	0.62
5.6	-9.4	-276.2	-287.6	-27.13	-2.91	5.64
6	-8.9	-239.2	-252.3	-8.49	1.60	6.10
6.4	-8.2	-206.2	-219.2	-2.19	1.43	3.73
6.8	-7.0	-173.0	-184.5	-0.31	0.68	1.86
7.2	-5.5	-141.0	-150.2	0.06	0.11	0.74
7.6	-4.1	-112.5	-119.5	0.13	-0.07	0.28

Genuine Nonadditive Effects from Supermolecular Approach

In general, the structure and energy of the Na_2B complex is determined by the two-body forces. A few comments about two-body energies are thus pertinent.

Gutowski¹⁰ determined the minimum of the lowest triplet state of the Na_2 interaction at the CCSD(T) level of theory with a large basis set. He obtained the well depth of $-809.66 \mu E_h$ at 5.129 \AA .

The minima of the lowest triplet states of the NaB interaction were found by us at the full UMP4(SDTQ) level with aug-cc-pVTZ basis set for B atom and Gutowski's basis for the Na atoms¹⁰. The NaB dimer shows extremely strong anisotropy. Both the Σ and Π states of the dimer have a completely different character. A very deep minimum of $-27\,974.0 \mu E_h$ of the Π state is located at 2.5 \AA (see also Simons *et al.*¹ for previous calculations of this diatom), while a very weak minimum of $-147.279 \mu E_h$ of the Σ state appears at 5.7 \AA . This must result in a large orientational nonadditivity in the Na_2B

TABLE XIII
Orientational part of BSSE for the NaB dimer with respect to the perpendicular state V_{Π}^{perp} calculated for monomer B in the A_1 and B_2 states

% error $R, \text{ \AA}$	$\Delta(\Pi)^a$			$\Delta(\text{BSSE-}A_1)^a$			$\Delta(\text{BSSE-}B_2)^a$		
	SCF	UMP2	UMP3	SCF	UMP2	UMP3	SCF	UMP2	UMP3
4	0.28	0.08	0.09	-0.18	-0.38	-0.31	0.43	0.24	0.22
4.2	0.28	0.07	0.09	-0.85	-0.59	-0.50	0.65	0.30	0.28
4.4	0.27	0.06	0.09	-2.05	-0.86	-0.75	1.04	0.37	0.37
4.6	0.29	0.05	0.09	-3.97	-1.17	-1.04	1.71	0.46	0.46
4.8	0.34	0.04	0.09	-6.66	-1.51	-1.35	2.68	0.56	0.56
5	0.48	0.03	0.09	-9.69	-1.82	-1.62	3.87	0.65	0.66
5.2	0.61	0.02	-1.82	-12.14	-2.05	-1.82	4.87	0.71	-1.82
5.4	1.01	0.02	0.08	-12.40	-2.14	-1.87	5.48	0.74	0.73
5.6	1.62	0.02	0.08	-9.52	-2.07	-1.77	5.33	0.72	0.69
6	3.46	0.01	0.05	4.77	-1.61	-1.30	3.03	0.55	0.50
6.4	6.29	0.01	0.04	19.29	-1.21	-0.89	1.96	0.41	0.35
6.8	7.80	-0.05	-0.03	17.83	-1.42	-1.07	4.45	0.41	0.32

^a For definitions, see Eqs (28)–(30).

trimer. Interestingly, the NaB interaction at the SCF level of theory turns out to be attractive for the Π state and repulsive for the Σ state.

An unusually large stabilization of the Π dimer is due to a reduction of the exchange repulsion by a perpendicular arrangement of the singly occupied p orbital, so that the attractive dispersion interaction can extend to smaller internuclear distances. This type of bonding has been reported by Breckenridge and collaborators^{43–45}, Sohlberg and Yarkony², and rationalized by Bililign *et al.*⁴⁶

The genuine nonadditivity in Na_2B and the pairwise additive interaction energy were obtained from supermolecular calculations, applying Eqs (2)–(5). For the B_1 state this was straightforward, as the NaB dimer and the trimer are related to the same, perpendicular arrangement of the p orbital (no orientational nonadditivity). To obtain the pair interactions in the A_1 and B_2 states, Eqs (14)–(19) were applied.

Table XIV lists supermolecular results for the Na_2B trimer in the states of the B_1 , B_2 , and A_1 symmetry, respectively. All results were obtained for the equilateral triangle arrangements at the SCF, UMP2, and UMP3 levels of theory. The interatomic distance R varied from 2.4 to 7.6 Å.

The first three columns consist of the total interaction energy of the trimer. The next three columns describe the two-body part of the interaction energy (including the orientational nonadditivity). The last three columns show the genuine three-body energy.

Table X shows the interaction energies of the NaB dimer in the symmetry states of the trimer (including the orientational nonadditivity).

The states of the trimer can be approximately related to the states of the dimer. The B_1 state is a purely Π state from the point of view of NaB, and thus it is the deepest. B_2 and A_1 correspond to a mixture of the Π and Σ states, but not with equal weight; A_1 corresponds more to Σ while B_2 corresponds more to Π . The ordering of states based on two-body forces only is $B_1 < B_2 < A_1$ for the studied ranges of interatomic distances. Consequently, the equilibrium structure of the Na_2B trimer in the B_1 state should be linear or nearly linear to optimize the equilibrium distances of all partners. For the same reason, the minimum of the B_2 state occurs for the triangle geometry (small Θ) with the interatomic angle limited by the Na_2 repulsion and the genuine nonadditivity effect, while for the A_1 state the minimum should be close to the B_1 state minimum (*i.e.*, it should be either linear or nearly linear).

The three-body nonadditive energy in the Na_2B trimer is a very important contribution to the interaction energy of the trimer, *cf.* Table XIV, and Figs 7 and 8. The neglect of the three-body energy would cause a large er-

TABLE XIV

The supermolecular results calculated for equilateral-triangle arrangement of the Na_2B trimer in the A_1 , B_1 , and B_2 states. Energy in μE_h

R	E_{int}			$E[2,3]$			$E[3,3]$		
	SCF	MP2	MP3	SCF	MP2	MP3	SCF	MP2	MP3
B_1 state									
2.5	-11459	-31756	-33052	16429	-18302	-21228	-27889	-13454	-11824
3	-13397	-32164	-33924	7574.5	-16994	-20312	-20972	-15169	-13611
4	1837.7	-4713.3	-6119.1	3122.7	-3304.2	-4731.7	-1285.3	-1409.1	-1387.4
4.4	1326.6	-2761.5	-3768.8	1865.9	-2320.0	-3363.5	-539.2	-441.5	-405.3
5	686.7	-1486.2	-2109.8	817.69	-1424.6	-2068.8	-130.94	-61.51	-40.95
6	178.83	-638.97	-920.67	187.32	-640.57	-926.76	-8.49	1.60	6.10
7.6	12.59	-178.08	-257.21	12.46	-178.01	-257.48	0.13	-0.07	0.28
B_2 state									
4	5437.6	927.70	-172.56	4390.6	-1264.9	-2588.4	1047.0	2192.6	2415.8
4.4	3126.8	-166.06	-1053.9	2576.3	-1231.7	-2227.5	550.44	1065.6	1173.6
5	1302.9	-684.31	-1285.4	1098.9	-1026.4	-1660.8	204.01	342.11	375.38
6	272.97	-533.40	-818.92	238.12	-577.06	-865.5	34.86	43.65	46.58
7.6				13.72	-177.14	-258.02			
A_1 state									
4	3528.0	-2519.3	-3957.8	6938.6	2874.9	1760.3	-3410.6	-5394.2	-5718.1
4.4	2551.5	-925.96	-1878.2	4012.8	1007.4	113.04	-1461.3	-1933.4	-1991.2
5	1244.1	-631.96	-1223.9	1678.6	-176.21	-783.59	-434.49	-455.75	-440.30
6	292.98	-467.06	-748.11	340.42	-436.62	-728.80	-47.44	-30.43	-19.31
7.6				17.85	-171.73	-255.23			

ror. For example, for the B_1 state the genuine MP3 nonadditivity amounts to about 30% for the van der Waals region ($R = 2.8 \text{ \AA}$), and it rapidly decreases to only 0.5% when the interatomic distance is twice as long (see Fig. 8). For the B_2 state almost one third of the attractive two-body interaction is cancelled by the three-body effects in the minimum region ($R =$

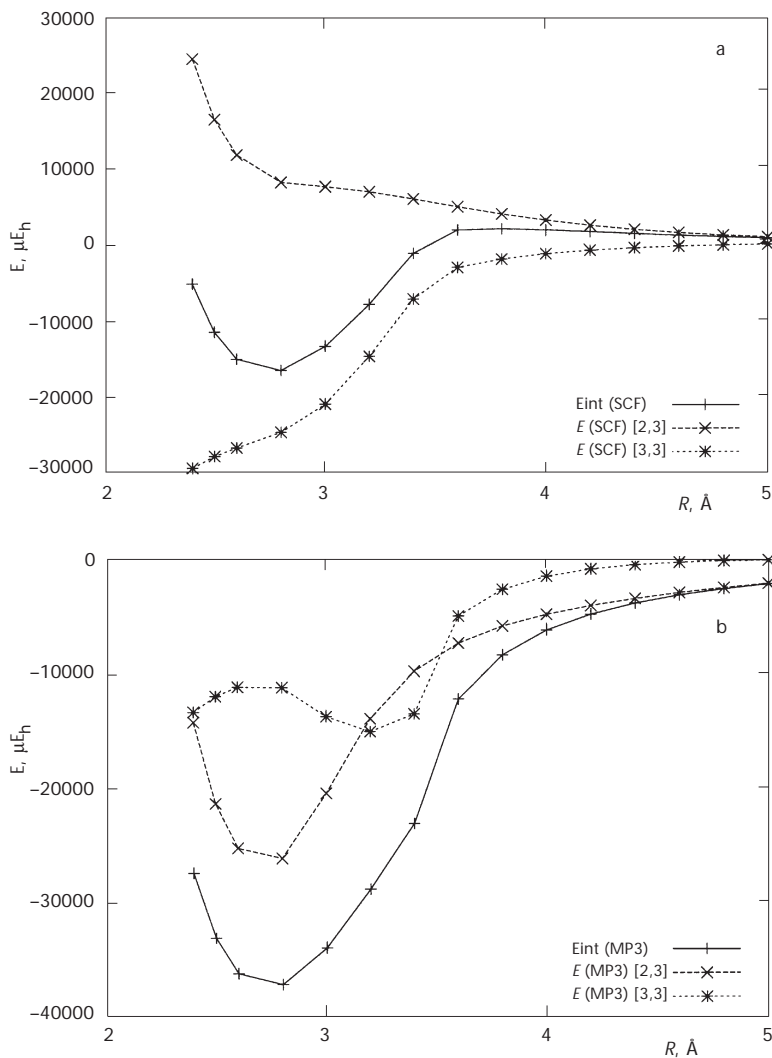


FIG. 8

Comparison of genuine nonadditivity with the whole interaction energy and its pairwise part in Na_2B . B_1 state, SCF level, $\Theta = 60^\circ$ (a); B_1 state, MP3 level, $\Theta = 60^\circ$ (b)

5.0 Å). For the A_1 state the nonadditivity is attractive and larger in size than the pairwise part of the interaction in the minimum region.

The nonadditive forces appear to be purely repulsive for the B_2 state. Interestingly, the B_1 and A_1 states are attractive for short distances, but repulsive in a long range, with a very weak maximum at about 6.0 and 6.8 Å, respectively.

One can see in Table XIV that the pairwise interaction energy at the SCF level is repulsive for all states. The total interaction energy at this level is repulsive for almost all regions except for the B_1 short-range regions. The total SCF interaction energy in the B_1 state exhibits unusual behavior for the studied regions: a shallow maximum at 3.8 Å is observed and a much deeper minimum at 2.8 Å. The latter minimum is due to the three-body SCF deformation that accompanies the Heitler–London exchange effect (see the next Section).

To summarize, the B_1 state is the least repulsive and the B_2 state the most repulsive. No minimum at the SCF level for the equilateral-triangle arrangement is observed.

The total interaction energy calculated at the correlated levels of theory has the opposite sign to that obtained at the SCF level for all distances, but the sequence of states is preserved.

The nonadditive forces reverse the order of the A_1 and B_2 levels for intermediate and short ranges. Within the two-body approximation, the B_2 state is lower than A_1 but allowing for nonadditivity reverses this order. Moreover, the minima for the A_1 and B_2 states change locations and depth. Allowing for the nonadditivity shortens the location of the minimum for the A_1 state from 5.4 to less than 4.0 Å, and lengthens the NaB distance for the B_2 symmetry from less than 4.0 to *ca* 4.8 Å. The minimum energy is much deeper for the A_1 symmetry of the Na_2B trimer and more shallow for the B_2 symmetry.

Perturbation Method: Three-Body Exchange, Induction, and Dispersion

Genuine Nonadditive Terms from Perturbation Treatment

Perturbation calculations employed TRURL codes³⁴, adapted to treat open-shells within the UHF approximation⁴⁷, including two- and three-body corrections. The program calculates the following three-body terms: the Heitler–London-exchange, the second- and third-order induction, and the third-order dispersion. The monomers are calculated with TCBS and the p

orbital is oriented as in the trimer. Therefore, one obtains only pure genuine three-body effects.

All computations were performed for the interatomic distance ranging from 2.5 to 7.6 Å of the equilateral triangle geometry of Na₂B. This range covers the minimum of pairwise interactions of (³Σ)Na₂ (5.2 Å) and (³Σ)NaB (5.7 Å), and is close to the minimum of (³Π)NaB (2.5 Å).

The three-body terms: Heitler–London exchange $\varepsilon_{\text{exch}}^{\text{HL}}$, third-order dispersion $\varepsilon_{\text{disp}}^{(30)}$, and induction $\varepsilon_{\text{ind},r}^{(30)}$ (iq-iq) are presented in Table XV and shown in Fig. 9. The latter term represents a part of the third-order induction term

TABLE XV
The IMPPT results for the equilateral-triangle arrangement of the Na₂B trimer in the A₁, B₁, and B₂ symmetry states. Energy in μE_h

<i>R</i> , Å	$\varepsilon_{\text{disp}}^{(30)}$	$\varepsilon_{\text{ind},r}^{(30)}$ (iq-iq)	$\varepsilon_{\text{exch}}^{\text{HL}}$	ΔE^{SCF}	$\Delta E_{\text{def}}^{\text{SCF}}$
A ₁ state					
2.5	1794.44	37399.44	-25650.64		
4	147.79	523.33	-3358.70	-3410.56	-51.86
4.4	74.91	176.07	-1702.90	-1461.30	241.60
5	27.51	48.85	-564.36	-434.49	129.86
6	5.60	9.97	-75.97	-47.44	28.53
7.6	0.59	1.03	-2.60		
B ₁ state					
2.5	1523.76	35524.95	-15840.15	-27888.68	-12048.53
4	137.11	785.26	-1372.40	-1285.26	87.14
4.4	70.39	274.91	-597.42	-539.21	58.21
5	26.26	64.37	-150.10	-130.94	19.16
6	5.50	8.63	-9.60	-8.49	1.11
7.6	0.61	0.76	0.22	0.13	-0.09
B ₂ state					
2.5	1628.11	33193.37	1532.60		
4	148.25	635.65	277.99	1046.99	769.00
4.4	76.17	219.61	180.62	550.44	369.82
5	28.42	53.56	86.78	204.01	117.24
6	5.97	8.33	19.95	34.86	14.91
7.6	0.67	0.83	1.22		

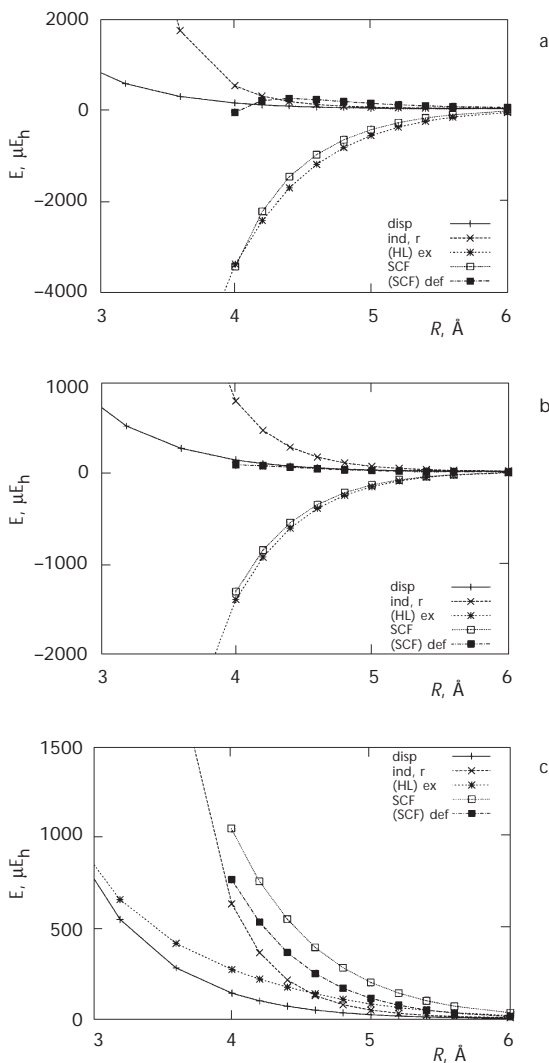


FIG. 9

The three-body nonadditive terms from the IMPPT calculation for the equilateral arrangement of Na_2B . The labels: disp, ind, r, (HL)ex, SCF, (SCF)def denote: $\epsilon_{\text{disp}}^{(30)}$, $\epsilon_{\text{ind},r}^{(30)}$ (iq-iq), Heitler-London exchange, SCF nonadditivity, and SCF deformation, respectively. A_1 state, $\Theta = 60^\circ$ (a); B_1 state, $\Theta = 60^\circ$ (b); B_2 state, $\Theta = 60^\circ$ (c)

which corresponds to the electrostatic interaction of the induced moments of the Na atoms generated by the electric field of B.

A major part of the nonadditivity is exchange in nature and is located in the SCF and the Heitler–London exchange terms. All other contributions appear to be secondary.

The Heitler–London exchange nonadditivity of the Na₂B system is negative for the A₁ and B₁ symmetries and positive for the B₂ symmetry. The exchange nonadditivity is in good agreement with the total supermolecular SCF nonadditivity. It has the same sign as the SCF nonadditivity, and has a comparable magnitude for all states.

The best agreement of the SCF nonadditivity is for the B₁ state, as the difference between SCF and Heitler–London results amounts to about 10%. Similarly, SCF non-additivity for the A₁ state differs by a few percentage points for short-range distances, but for long-range distances it amounts to as much as half of the exchange effects. The B₂ state SCF nonadditivity is about twice as big as the Heitler–London exchange for the studied distances.

Although the main part of the nonadditivity is of the exchange nature, the induction and dispersion terms cannot be neglected, especially for A₁ and B₂, for which the correlated MP3 nonadditivity is about twice as big as the SCF nonadditivity. Moreover, the MP3 long-range interaction in B₁ state exhibits the maximum at 6 Å, which cannot be explained by exchange terms, which behave monotonically.

In general, the MP3 nonadditivity is better recovered by the sum of SCF and dispersion three-body terms for smaller distances. The sum of dispersion, induction and Heitler–London exchange terms agrees better with MP3 for the long-range distances. Both models recover a shallow maximum of the interaction energy of the B₁ state at about 6 Å, and a monotonic decrease in the interaction energy for the B₂ state with increasing *R*.

The Exchange Nonadditivity and Pseudodimer Treatment of Na₂B

In this Section decomposition of the first-order exchange energy into the single-exchange SE and triple-exchange TE components is carried out by means of the pseudodimer approach^{29,34,48}. The electrostatic model of the SE term in Na₂B is discussed and analyzed.

The Heitler–London exchange nonadditivity was partitioned into the TE term and various SE components. The total SE term, which is denoted here as SE_tot, is divided into three parts. Each of the SE terms represents the exchange of electrons between the various two monomers in the trimer. The symbol in the bracket labels monomers in which electrons are exchanged.

For example, $SE_{\text{Na..Na}}$ represents the exchange of electrons between two Na atoms coupled with the electrostatic interaction with the B atom^{48,49}.

Detailed information about partial and total SE terms, the TE term, and the total Heitler–London exchange nonadditivity is presented in Table XVI.

The TE term is negative for all studied distances and for each symmetry. For the B_2 symmetry, it decreases most rapidly, with the highest negative value for R of 2.5 Å, and the lowest absolute value for $R = 7.6$ Å.

TABLE XVI

The SE and TE contributions to the Heitler–London nonadditivity for the equilateral-triangle arrangement of Na_2B in the A_1 , B_1 , and B_2 states

R , Å	$\epsilon_{\text{exch}}^{\text{HL}}$	$SE_{\text{(B..Na)}}$	$SE_{\text{(Na..Na)}}$	SE_{tot}	TE
A_1 state					
2.5	-25650.64	10377.91	11833.42	32589.25	-58239.88
4	-3358.70	342.53	321.13	1006.19	-4364.89
4.4	-1702.90	124.08	38.48	286.63	-1989.53
5	-564.36	25.38	-46.23	4.53	-568.88
6	-75.97	1.56	-20.32	-17.20	-58.76
7.6	-2.60	0.01	-1.56	-1.54	-1.06
B_1 state					
2.5	-15840.15	3130.50	14779.79	21040.80	-36880.94
4	-1372.40	34.20	1056.00	1124.39	-2496.79
4.4	-597.42	10.19	474.84	495.21	-1092.63
5	-150.10	1.67	137.83	141.17	-291.27
6	-9.60	0.07	16.83	16.98	-26.57
7.6	0.22	0.00	0.62	0.62	-0.40
B_2 state					
2.5	1532.61	444.40	18333.19	19154.96	-17622.35
4	277.99	-76.45	1487.59	1336.01	-1058.02
4.4	180.62	-28.74	699.62	642.43	-461.81
5	86.78	-5.79	218.59	207.02	-120.24
6	19.95	-0.33	30.37	29.71	-9.76
7.6	1.22	0.00	1.32	1.31	-0.09

The ordering of states is $B_2 > B_1 > A_1$. The $SE_{(Na..Na)}$ exchange effect is positive for the B_1 and B_2 symmetry but negative at the long range of the A_1 symmetry. For the B_2 symmetry, it is about twice as repulsive as for the B_1 symmetry.

Except for the short range of the A_1 state, the anisotropy of $SE_{(Na..Na)}$ agrees qualitatively well with the model of the exchange quadrupole interacting with a third species. In our case, such an exchange quadrupole interacts with the permanent quadrupole located at the B center. This permanent quadrupole moment on B is due to the axial symmetry of the electronic density of the singly-occupied p orbital centered at the B atom.

The plausible explanation of a dramatic change of the sign of $SE_{(Na..Na)}$ for the A_1 symmetry for distances shorter than 4.6 Å is a significant increase of higher DE terms. These terms are proportional to the fourth power of the overlap integral and could be of the opposite sign to the SE term:

$$SE = -\langle Vc_2 \rangle + \langle c_2 \rangle \langle V \rangle \quad (33)$$

$$DE \cong -SE \cdot \langle c_2 \rangle, \quad (34)$$

where the c_2 is operator of the exchange of electrons and V is electrostatic Coulomb operator. An additional argument is that the change of sign occurs for distances smaller than the van der Waals radius of the Na atom (equal to the equilibrium distance of the Na–Na potential), where the exchanges of inner electrons should be more significant.

The term $SE_{(Na..B)}$ exhibits interesting orientational anisotropy (Fig. 10). It may be interpreted in terms of exchange and overlapping of Na and B half-filled orbitals. For the B_1 state, the overlap integral of the boron p orbital with the s orbital of any of the Na atoms vanishes due to the Π symmetry. This results in a considerable decrease in the exchange effect $SE_{(Na..B)}$ with respect to other symmetry states. Thus the $SE_{(Na..B)}$ term in the case of the B_1 state is over one order of magnitude lower than for the A_1 state. The $SE_{(Na..B)}$ term of the B_1 state may be thought of as an indicator of how extensive the inner electron cloud of boron is (the rapid increase in $SE_{(Na..B)}$ begins with penetration of the inner shell of B by the Na electron cloud).

The absolute values of the Na..B exchanges in the B_2 state are also much lower than for the A_1 state. This is caused by a greater similarity of that state to the Π symmetry rather than to the Σ symmetry. Moreover, the $SE_{(Na..B)}$ term for each state is much lower than the relevant $SE_{(Na..Na)}$ term.

Electrostatic Model of SE

Historically, the Jansen effective-electron model of exchange effects was the first model to explain the exchange nonadditivity²⁵. The idea is based on the electrostatic interaction of an exchange quadrupole located at the center of mass of two atoms with a permanent multipole located on the third atom (see also ref.²⁶ for extensions of this model).

An electrostatic model involving the interaction of the exchange quadrupole on Na₂ with the quadrupole moment of B predicts attractive exchange energy for A₁ and repulsive for B₁ and B₂. Moreover, the repulsive effect for B₂ should be greater than the repulsive effect for B₁. Figure 11 shows the orientational dependence between quadrupole on B and the

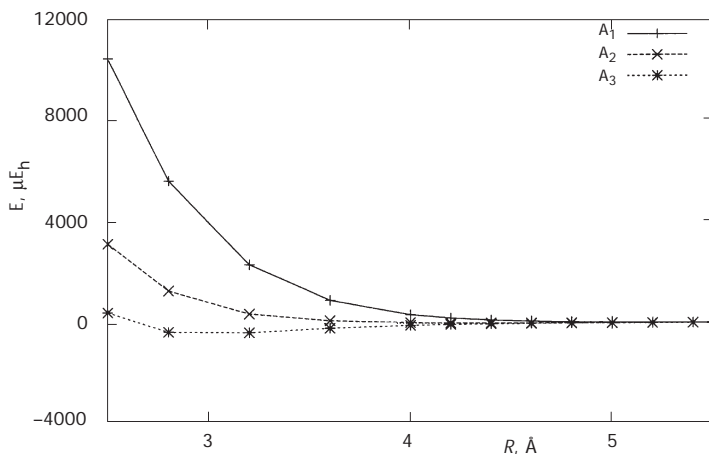


FIG. 10

The SE_(Na..B) exchange terms for the A₁, B₁, and B₂ symmetry states of Na₂B. $\Theta = 60^\circ$

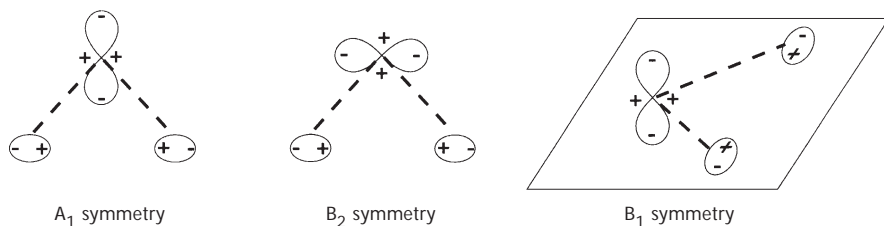


FIG. 11

The SE_(Na..Na) term could be intuitively understood as the electrostatic interaction energy between a permanent quadrupole located at the B atom with the exchange quadrupole in the middle of the Na₂ dimer

exchange quadrupole on Na_2 . Such a model qualitatively explains the behavior of the $\text{SE}_-(\text{Na-Na})$ term (see Table XVI) with respect to the electronic state.

SUMMARY AND CONCLUSIONS

The Na_2B , Na_3 and H_3 trimers in the lowest quartet states were studied by *ab initio* methods, using both the supermolecular approach and the intermolecular Møller-Plesset perturbation theory. Partitioning of the non-additive contribution into the orientational two-body part and the genuine three-body part was proposed.

The lowest quartet state of the Na_3 trimer and all the three lowest quartet states of the Na_2B trimer were found to be bound. The geometries of these clusters are essentially determined by two-body forces. Thus, the sodium trimer is an equilateral triangle. By way of contrast, the Na_2B trimer is either (almost) collinear (for the quartet states related to the B_1 and B_2 symmetries of the $2p$ boron orbital) or triangular (for the quartet state related to the A_1 symmetry of the $2p$ boron orbital). This diversity results from the orientational nonadditivity, and is due to the interplay between the Π and Σ states of the NaB moieties. The former state is strongly bound with the bond length close to 2.5 \AA , whereas the latter state reveals a typically weak van der Waals bond with the long equilibrium distance of 5.7 \AA . As a consequence, the lowest quartet state of Na_2B is collinear, the p -symmetry singly occupied orbital being perpendicular to the Na_2B triangle (B_1 symmetry).

In the title metal trimers, in the region of the van der Waals minima, the genuine nonadditivity is very important, and amounts to 30% in Na_2B , and up to 70% in Na_3 . The leading nonadditive term is the triple-exchange Heitler-London exchange term. For triangular arrangements it considerably enhances the overall stabilization. The single-exchange term and the SCF deformation play only a secondary role. The dispersion nonadditivity is negligible.

The isotropic part of BSSE is large and must be corrected by the counterpoise method. The anisotropic contribution to BSSE is practically negligible.

M. M. Szcześniak and G. Chałasiński thank the National Science Foundation (grant No. CHE-0078533) for support. International collaboration was supported by NATO through the Linkage Grant CRG.LG 974215. J. Jakowski and G. Chałasiński acknowledge support by the Polish Committee for Scientific Research KBN (grant 3 T09A 112 18).

REFERENCES

1. Boldyrev A. I., Gonzales N., Simons J.: *J. Phys. Chem.* **1994**, *98*, 9931.
2. Sohlberg K., Yarkony D. R.: *J. Phys. Chem.* **1997**, *101*, 3166.
3. Boatz J. M., Fajardo M. E.: *J. Chem. Phys.* **1994**, *101*, 3472.
4. Kiljunen T., Eloranta J., Ahokas J., Kunttu H.: *J. Chem. Phys.* **2001**, *114*, 7144.
5. Kiljunen T., Eloranta J., Ahokas J., Kunttu H.: *J. Chem. Phys.* **2001**, *114*, 7157.
6. Snyder J. A., Jaffe J. E., Gutowski M., Lin Z., Hess A. C.: *J. Chem. Phys.* **2000**, *112*, 3014.
7. Feurestein B., Grum-Grzhimailo A. N., Bartschat K., Mehlhorn W.: *J. Phys. B: At., Mol. Opt. Phys.* **1999**, *32*, 3727.
8. Barrios R., Skurski P., Rak J., Gutowski M.: *J. Chem. Phys.* **2000**, *113*, 8961.
9. Jagielska A., Moszyński R., Piela L.: *J. Chem. Phys.* **1999**, *110*, 947.
10. Gutowski M.: *J. Chem. Phys.* **1999**, *110*, 4695.
11. Higgins J., Hollebeck T., Reho J., Ho T.-S., Lehmann K. K., Rabitz H., Scoles G., Gutowski M.: *J. Chem. Phys.* **2000**, *112*, 5751.
12. Yang X., Hwang E., Dagdigian P., Yang M., Alexander M. H.: *J. Chem. Phys.* **1995**, *103*, 2779.
13. Yang X., Hwang E., Dagdigian P.: *J. Chem. Phys.* **1996**, *104*, 8165.
14. Yang X., Hwang E., Dagdigian P.: *J. Chem. Phys.* **1996**, *104*, 599.
15. Yang X., Dagdigian P.: *J. Chem. Phys.* **1997**, *106*, 6596.
16. Alexander M. H., Walton A. R., Yang M., Yang X., Hwang E., Dagdigian P.: *J. Chem. Phys.* **1997**, *106*, 6320.
17. Krumrine J. R., Alexander M. H., Yang X., Dagdigian P.: *J. Chem. Phys.* **2000**, *112*, 5037.
18. Szcześniak M. M., Chałasiński G. in: *Molecular Interactions* (S. Scheiner, Ed.), p. 45. Wiley, Chichester 1997.
19. Chałasiński G., Szcześniak M. M.: *Chem. Rev. (Washington, D. C.)* **1994**, *94*, 1723.
20. Jeziorski B., Moszyński R., Szalewicz K.: *Chem. Rev. (Washington, D. C.)* **1994**, *94*, 1887.
21. Alonso J., Lopez M. in: *Theory of Atomic and Molecular Clusters* (J. Jellinek, Ed.). Springer-Verlag, Berlin-Heidelberg 1999.
22. Tang K. T., Norbeck J. M., Certain P. R.: *J. Chem. Phys.* **1976**, *64*, 3063.
23. Korona T., Moszyński R., Jeziorski B.: *J. Chem. Phys.* **1996**, *105*, 8178.
24. Kleinkathöfer U., Sachse T. I., Tang K. T., Toennies J. P., Yiu C. L.: *J. Chem. Phys.* **2000**, *113*, 984.
25. Jansen L.: *Phys. Rev.* **1962**, *125*, 1798.
26. Wheatley R. J.: *Mol. Phys.* **1995**, *84*, 899.
27. Kleinkathöfer U., Tang K. T., Toennies J. P., Yiu C. L.: *J. Chem. Phys.* **1999**, *111*, 3377.
28. Chałasiński G., Szcześniak M. M.: *Chem. Rev.* **2000**, *100*, 4227.
29. Chałasiński G., Rak J., Szcześniak M. M., Cybulski S. M.: *J. Chem. Phys.* **1997**, *106*, 3301.
30. Woon D. E., Dunning T. H.: *J. Chem. Phys.* **1994**, *100*, 2975.
31. Dunning T. H.: *J. Chem. Phys.* **1989**, *90*, 1007.
32. Kendall R. A., Dunning T. H., Harrison R. J.: *J. Chem. Phys.* **1992**, *96*, 6796.
33. Frisch M. J., Trucks G. W., Schlegel H. B. *et al.*: *GAUSSIAN 98*, Revision A.7. Gaussian, Inc., Pittsburgh (PA) 1998.
34. Cybulski S. M.: *TRURL-94 Package*. Rochester (MI) 1994.
35. Yourshaw I., Zhao Y., Neumark D. M.: *J. Chem. Phys.* **1996**, *105*, 351.
36. Sando K. M., Erickson G. J., Binning R. C., Jr.: *J. Phys. B: At., Mol. Opt. Phys.* **1979**, *12*, 2697.

37. Erickson G. J., Sando K. M.: *Phys. Rev. A: At., Mol., Opt. Phys.* **1980**, 22, 1500.
38. Aquilanti V., Liuti G., Pirani F., Vecchiocattivi F.: *J. Chem. Soc., Farraday Trans. 2* **1989**, 85, 955.
39. Naumkin F. Y., Knowles P. J.: *J. Chem. Phys.* **1995**, 103, 3392.
40. Danilychev A. V., Apkarian V. A.: *J. Chem. Phys.* **1994**, 100, 5556.
41. Jakowski J.: *Ph.D. Thesis*. Warsaw 2002.
42. Reid R. H. G.: *J. Phys. B: At., Mol. Opt. Phys.* **1973**, 6, 2018.
43. Massick S., Breckenridge W. H.: *J. Chem. Phys.* **1996**, 104, 7784.
44. Massick S., Breckenridge W. H.: *J. Chem. Phys.* **1996**, 105, 6154.
45. Duval M.-C., D'Azy O. B., Breckenridge W. H., Jouvet C.: *J. Chem. Phys.* **1986**, 85, 6324.
46. Bililign S., Gutowski M., Simons J., Breckenridge W. H.: *J. Chem. Phys.* **1984**, 100, 8212.
47. Cybulski S. M.: Unpublished results.
48. Jakowski J., Chałasiński G., Szcześniak M. M., Cybulski S. M.: *Chem. Phys.* **1998**, 239, 573.
49. Cooper A. R., Hutson J. M.: *J. Chem. Phys.* **1993**, 98, 5337.
50. Stone A. J.: *The Theory of Intermolecular Forces*. Clarendon Press, Oxford 1996.
51. Stone A. J., Alderton M.: *Mol. Phys.* **1985**, 56, 1047.
52. Chałasiński G., Szcześniak M. M., Cybulski S. M.: *J. Chem. Phys.* **1990**, 92, 2481.
53. Chałasiński G., Cybulski S. M., Szcześniak M. M., Scheiner S.: *J. Chem. Phys.* **1989**, 91, 7048.